



Research paper

An experimental and theoretical investigation of lanthanide complexes [Ln = Nd, Yb, Eu, Dy and Tb] with 4-((2-hydroxy-naphthalen-1-yl)methylene amino)benzenesulfonamide ligand

Sikandar Paswan^a, Nitesh Jaiswal^b, Vishnu Kumar Modanawal^a, Manoj Kumar Patel^a, Rana Krishna Pal Singh^{a,*}

^a Synthetic Inorganic and Metallo-Organic Research Laboratory, Department of Chemistry, University of Allahabad, Prayagraj 211002, Uttar Pradesh, India

^b Department of Chemistry, Prof. Rajendra Singh (Rajju Bhaiya) Institute of Physical Sciences for Study and Research, Veer Bahadur Singh Purvanchal University, Jaunpur 222003, Uttar Pradesh, India



ARTICLE INFO

Keywords:

Lanthanide complexes
Schiff base
DFT
Fluorescence studies
Antibacterial studies

ABSTRACT

Reaction of lanthanide(III) salts with N, O donors 4-((2-hydroxynaphthalen-1-yl)methyleneamino)benzenesulfonamide (L) Schiff base ligand afforded five new mononuclear lanthanide complexes of type $[\text{Ln}(\text{NO}_3)_2(\text{L})(\text{H}_2\text{O})_2](\text{H}_2\text{O})_x$ {where Ln = Nd (1), x = 2, Yb (2), x = 1, Eu (3), x = 2, Dy (4), x = 1, Tb (5), x = 2}. These newly synthesized complexes were characterized by elemental analysis, molar conductance, FT-IR, UV-Vis spectroscopy and mass spectrometry. The thermal behavior of complexes was studied by TGA technique. The computational calculations using density functional theory (DFT) of ligand and their lanthanide complexes were performed to obtain optimized molecular geometry, the highest occupied molecular orbital (HOMO), the lowest unoccupied molecular orbital (LUMO) and other parameters. The fluorescence studies reveal that emission spectra of lanthanide complexes show the characteristic luminescence due to lanthanide ions which indicates that Schiff base ligand can sensitize the Ln(III) ions. The Schiff base and their lanthanide complexes were screened for their *in vitro* antibacterial studies against *Escherichia coli* (ATCC 25922), *Staphylococcus aureus* (ATCC 29213), *Klebsiella pneumoniae* (BAA 1705), *Acinetobacter baumannii* (BAA 1605) and *Pseudomonas aeruginosa* (ATCC 27853). The results exhibit that the antibacterial activity of Ln(III) complexes was greater than the free Schiff base ligand.

1. Introduction

The growing demand of luminescent materials for different societal applications has been witnessed in recent times. The luminescence and magnetic features of lanthanide complexes motivated the researcher for its exploration. The design and synthesis of lanthanide complexes with organic ligands including Schiff bases emerged as an important research area in recent times [1–4]. The existence of long-lived excited states of trivalent lanthanide ions (Ln^{3+}) produces the luminescence properties in lanthanide complexes. These photophysical properties of lanthanide complexes could be tuned and enhanced with the help of rationally designed ligands. The emerging interest of chemists towards research in the lanthanide complexes is due to their interesting structures [5,6] and a wide range of potential applications in biological sectors, catalysis, luminescence and magnetic properties [7–10].

Sulfonamides were the first drugs used as preventive and

therapeutic agents against different diseases [11–14]. Sulfur donor Schiff base ligands play an important role in metal coordination chemistry due to its important biological properties including antibacterial, anti-toxicity, antifungal and antitumor properties [15,16]. The biological activities of metal complexes in several cases improved significantly on the addition of sulfonamide derivative ligands to metal salts rationally. The metal complexes of sulfonamide derivatives ligands have shown significant potential against cancer cell lines and other biological activities [17]. The interesting coordination chemistry of lanthanide metals with N, O donor Schiff base ligands and their applications in different scientific areas including chemical, medical and industrial sectors make enough for their importance and fascinate the chemist for the synthesis of new complexes [18].

Due to the above promising facts and our continued interest [19], an attempt was made to investigate the synthesis, characterization and antimicrobial properties of lanthanide (III) Schiff base complexes. In

* Corresponding author.

E-mail address: rkp.singh@rediffmail.com (R.K.P. Singh).

our investigation, we have utilized the sulfanilamide and 2-hydroxy-1-naphthaldehyde derive Schiff base ligand (L), to prepare a series of mononuclear lanthanide derivatives (1–5) $[\text{Ln}(\text{III})(\text{L})(\text{NO}_3)_2(\text{H}_2\text{O})_2]$ ($\text{Ln} = \text{Nd}, \text{Dy}, \text{Eu}, \text{Yb}, \text{Tb}$; $\text{L} = 4-((2\text{-hydroxynaphthalen-1-yl})\text{methyleneamino})\text{benzenesulfonamide}$). These complexes were investigated by elemental analysis, molar conductance, FT-IR and UV-Vis spectroscopy, mass spectrometry and thermal technique. Theoretical investigation using the DFT method was performed to get validation of experimental data. The fluorescence activity and biological properties of these complexes were also investigated.

2. Experimental

2.1. Materials and reagent

$\text{Nd}(\text{NO}_3)_3 \cdot 6\text{H}_2\text{O}$, $\text{Dy}(\text{NO}_3)_3 \cdot 5\text{H}_2\text{O}$, $\text{Yb}(\text{NO}_3)_3 \cdot 5\text{H}_2\text{O}$, $\text{Eu}(\text{NO}_3)_3 \cdot 5\text{H}_2\text{O}$, $\text{Tb}(\text{NO}_3)_3 \cdot x\text{H}_2\text{O}$, sulfanilamide, 2-hydroxy-1-naphthaldehyde were bought from Sigma Aldrich and utilized without any further purification. AR grade solvents were utilized for the production and recrystallization of compounds.

2.2. Physical measurements

The fundamental (C, H and N) analyses have been performed on CHN-932 Perkin-Elmer 7300 DV elemental analyzer. In KBr pellets and on a Perkin-Elmer 1000 FT-IR spectrophotometer the FT-IR spectrum has been performed from 4000 to 400 cm^{-1} region. The mass spectra (HRMS) were taken in ESI mode on Xevo G2-S Q ToF. Under the inert N_2 atmosphere, on STA 6000 Perkin Elmer instrument the thermogravimetric analyses (TGA) and differential thermal analyses (DTA) of complexes have been recorded. UV-Vis spectra were measured within the DMSO solution at temperature and λ_{max} was taken in (nm) by UV-1800 Shimadzu UV spectrophotometer. The fluorescence analysis was carried out by the Perkin Elmer LS-55 fluorescence spectrophotometer with a spectral resolution of $\sim 0.5\text{ nm}$, slit widths $\sim 9\text{ mm}$, quartz cell 1 cm .

2.3. Synthesis of Schiff base ligand

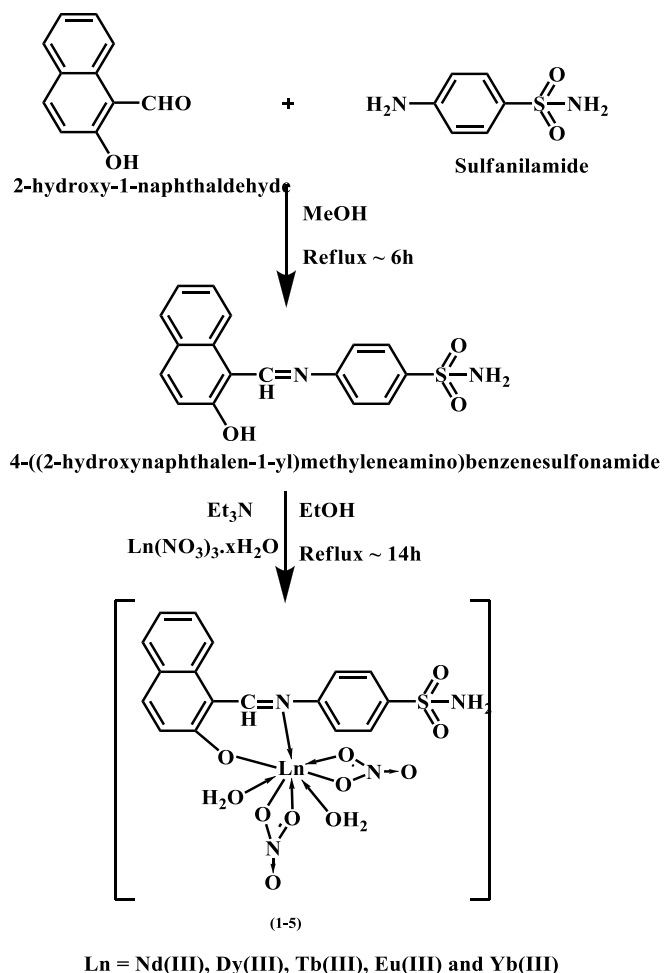
The ligand 4-((2-hydroxynaphthalen-1-yl)methyleneamino)benzenesulfonamide [20,21] (L) has been synthesized by the reaction of sulfanilamide and 2-hydroxy-1-naphthaldehyde in 1:1 M ratio(s). The 5.22 mmol each of Sulfanilamide and 2-hydroxy-1-naphthaldehyde were mixed in $\sim 35\text{ cm}^3$ methanol solvent and refluxed for $\sim 5\text{ h}$. The resulting yellow product washed with cold methanol and dried at room temperature. Finally recrystallization of this compound with hot methanol gives analytically pure powdered yellow product.

4-((2-hydroxynaphthalen-1-yl)methyleneamino)benzenesulfonamide (L) Yield: 82%, yellow powder, m.p. 281–83 °C, Elem. Anal. for $\text{C}_{17}\text{H}_{14}\text{N}_2\text{O}_3\text{S}$, Calcd. C, 62.56; H, 4.32; N, 8.58 Found: C, 62.48; H, 4.26; N, 8.51%. TOF-MS: Calcd. 326.07, Found: 327.42. IR (KBr, cm^{-1}): 3320 $\nu(\text{-OH})$; 3294 $\nu(\text{-NH}_2)$; 1630 $\nu(\text{C=N})$; 1465 $\nu(\text{Ar-O})$; 1360, 1157 $\nu(\text{SO}_2)$; 971 $\nu(\text{S-N})$; 835 $\nu(\text{C-S})$. UV-Vis (DMSO, λ_{max}): 380 ($\pi \rightarrow \pi^*$), 435, 457 ($n \rightarrow \pi^*$) nm.

2.4. General procedure for the synthesis of lanthanide complexes

The preparation of all Ln(III) complexes $[\text{Ln}(\text{L})(\text{NO}_3)_2(\text{H}_2\text{O})_2](\text{H}_2\text{O})_x$ (1–5) have been done by the following procedure.

The Schiff base (0.537 g, 1.64 mmol) was dissolved in ethanol (20 mL) and subsequently an ideal ethanolic solution of $\text{Nd}(\text{NO}_3)_3 \cdot 6\text{H}_2\text{O}$ (0.722 g, 1.64 mmol) was added to this solution. After few minutes, KOH in ethanol was added to the resulting solution and stirring for 24 h at 40 °C. A deep yellow color solution was obtained. The complex was dried by vacuum rotavapor to give yellow solid which is purified by ethanol solution (Scheme 1).



Scheme 1. Synthetic route for the preparation of ligand and Ln(III) complexes.

2.4.1. $[\text{Nd}(\text{L})(\text{NO}_3)_2(\text{H}_2\text{O})_2](\text{H}_2\text{O})_2$ (1)

Yield: 69%, yellow solid, m.p. 260–65 °C, Elem. Anal. for $\text{C}_{17}\text{H}_{17}\text{N}_4\text{O}_{11}\text{Nd}$, Calcd. C, 32.43; H, 2.72; N, 8.90 Found: C, 32.37; H, 2.66; N, 8.82%. TOF-MS: Calcd. 626.87, Found: 625.42. IR (KBr, cm^{-1}): 3445 $\nu(\text{H}_2\text{O})$; 3291 $\nu(\text{NH}_2)$; 1594 $\nu(\text{C=N})$; 1437 $\nu(\text{Ar-O})$; 1494, 1135, 820, 1287 $\nu(\text{NO}_3)$; 1365, 1150 $\nu(\text{SO}_2)$; 963 $\nu(\text{S-N})$; 830 $\nu(\text{C-S})$; 547 $\nu(\text{Nd-O})$; 468 $\nu(\text{Nd-N})$; UV-Vis (DMSO, λ_{max}): 384 ($\pi \rightarrow \pi^*$), 438, 462 ($n \rightarrow \pi^*$) nm. Molar conductance (DMF, Λ_m): $102\ \Omega^{-1}\text{ cm}^2\text{ mol}^{-1}$.

2.4.2. $[\text{Yb}(\text{L})(\text{NO}_3)_2(\text{H}_2\text{O})_2](\text{H}_2\text{O})$ (2)

Yield: 72%, brown solid, m.p. 258–62 °C, Elem. Anal. for $\text{C}_{17}\text{H}_{17}\text{N}_4\text{O}_{11}\text{SYb}$, Calcd. C, 31.01; H, 2.60; N, 8.51 Found: C, 30.91; H, 2.51; N, 8.46%. TOF-MS: Calcd. 659.00, Found: 658.11. IR (KBr, cm^{-1}): 3390 $\nu(\text{H}_2\text{O})$; 3290 $\nu(\text{NH}_2)$; 1594 $\nu(\text{C=N})$; 1444 $\nu(\text{Ar-O})$; 1502, 1050, 827, 1180 $\nu(\text{NO}_3)$; 1358, 1157 $\nu(\text{SO}_2)$; 971 $\nu(\text{S-N})$; 835 $\nu(\text{C-S})$; 540 $\nu(\text{Yb-O})$; 461 $\nu(\text{Yb-N})$; UV-Vis (DMSO, λ_{max}): 386 ($\pi \rightarrow \pi^*$), 440, 463 ($n \rightarrow \pi^*$) nm. Molar conductance (DMF, Λ_m): $101\ \Omega^{-1}\text{ cm}^2\text{ mol}^{-1}$.

2.4.3. $[\text{Eu}(\text{L})(\text{NO}_3)_2(\text{H}_2\text{O})_2](\text{H}_2\text{O})_2$ (3)

Yield: 66%, dark brown, m.p. 261–62 °C, Elem. Anal. for $\text{C}_{17}\text{H}_{17}\text{N}_4\text{O}_{11}\text{SEu}$, Calcd. C, 32.04; H, 2.69; N, 8.79 Found: C, 31.98; H, 2.60; N, 8.71%. TOF-MS: Calcd. 637.98, Found: 636.73. IR (KBr, cm^{-1}): 3505 $\nu(\text{H}_2\text{O})$; 3291 $\nu(\text{NH}_2)$; 1602 $\nu(\text{C=N})$; 1447 $\nu(\text{Ar-O})$; 1502, 1043, 827, 1287 $\nu(\text{NO}_3)$; 1355, 1150 $\nu(\text{SO}_2)$; 978 $\nu(\text{S-N})$; 831 $\nu(\text{C-S})$; 540 $\nu(\text{Eu-O})$; 460 $\nu(\text{Eu-N})$; UV-Vis (DMSO, λ_{max}): 356 ($\pi \rightarrow \pi^*$), 425, 464 ($n \rightarrow \pi^*$) nm. Molar conductance (DMF, Λ_m):

$94 \Omega^{-1} \text{ cm}^2 \text{ mol}^{-1}$.

2.4.4. [Dy(L)(NO₃)₂(H₂O)₂](H₂O) (4)

Yield: 71%, black solid, m.p. 270–74 °C, Elem. Anal. for C₁₇H₁₇N₄O₁₁SDy, Calcd. C, 31.51; H, 2.64; N, 8.65 Found: C, 31.44; H, 2.55; N, 8.58%. TOF-MS: Calcd. 648.99, Found: 648.23. IR (KBr, cm⁻¹): 3530 ν(H₂O); 3290 ν(NH₂); 1602 ν(C=N); 1447 ν(Ar-O); 1494, 1035, 820, 1275 ν(NO₃); 1355, 1157 ν(SO₂); 963 ν(S-N); 835 ν(C-S); 535 ν(Dy-O); 460 ν(Dy-N); UV-Vis (DMSO, λ_{max}): 363 (π → π*), 434, 463 (n → π*) nm. Molar conductance (DMF, Λ_m): 105 Ω⁻¹ cm² mol⁻¹.

2.4.5. [Tb(L)(NO₃)₂(H₂O)₂](H₂O)₂ (5)

Yield: 67%, dark brown, m.p. 240–46 °C, Elem. Anal. for C₁₇H₁₇N₄O₁₁STb, Calcd. C, 31.69; H, 2.66; N, 8.70 Found: C, 31.59; H, 2.57; N, 8.61%. TOF-MS: Calcd. 634.99, Found: 633.09. IR (KBr, cm⁻¹): 3510 ν(H₂O); 3290 ν(NH₂); 1597 ν(C=N); 1440 ν(Ar-O); 1498, 1040, 821, 1285 ν(NO₃); 1356, 1155 ν(SO₂); 970 ν(S-N); 830 ν(C-S); 541 ν(Tb-O); 462 ν(Tb-N); UV-Vis (DMSO, λ_{max}): 385 (π → π*), 438, 463 (n → π*) nm. Molar conductance (DMF, Λ_m): 97 Ω⁻¹ cm² mol⁻¹.

2.5. Computational method

Gaussian 09 program [22] was used to perform the computational investigation of newly synthesized complexes. The optimized geometry of the lanthanide complexes was obtained using density functional theory (DFT) methods at B3LYP level [23] with SDD (d, f) basic set [24]. The B3LYP/SDD employs three-parameter Becke exchange functional, B3 [25], the Lee-Yang-Parr nonlocal correctional functional LYP and the polarized SDD basis set [26–28].

2.6. In vitro antibacterial study

The ligand (L) and their Ln(III) complexes were screened for *in vitro* antibacterial testing against different pathogens *Escherichia coli* (ATCC 25922), *Pseudomonas aeruginosa* (ATCC 27853), *Acinetobacter baumannii* (BAA 1605), *Klebsiella pneumoniae* (BAA 1705) characterized into *gram negative* and *Staphylococcus aureus* (ATCC 29213) characterized into *gram positive* by using micro broth dilution assay. These pathogens were regularly cultivated on Mueller-Hinton broth Agar (MHA). Before the experiment, a single colony was picked from the MHA plate, inoculated in Mueller-Hinton cation supplemented broth II (CA-MHB) and incubated overnight at 37 °C. The stock solution (1 mg mL⁻¹) of the drug samples was prepared in the DMSO solution which was diluted to 100 μg mL⁻¹ with sterilized distilled water. The Minimum Inhibitory Concentration (MIC) was determined as per the Clinical Laboratory Standards Institute (CLSI) guidelines [29,30]. MIC is defined as the minimum amount of compounds at which observable bacterial growth is repressed. The optical density (OD₆₀₀) of the cultures was measured, followed by dilution for 1 × 10⁶ CFU/mL. This inoculum was added into a series of test wells in a microtitre plate that contained various concentrations of the compound under test ranging from 64 to 0.03 mg/mL. The controls i.e., cells alone and media alone (without compound & cells) and levofloxacin used as a reference standard. The plates were incubated at 37 °C for 24 h followed by observation of MIC were made. MIC determinations were performed independently using duplicate samples each time [31].

3. Results and discussion

In the existing investigation, five new Ln(III) complexes of synthesized ligand (L) were prepared and characterized by different spectroscopic techniques. The synthesis of ligand was done by the one-step condensation of sulfanilamide and 2-hydroxy-1-naphthaldehyde. The lanthanide complexes formulated as [Ln(NO₃)₂(L)(H₂O)₂](H₂O)_x

{where Ln = Nd (1), x = 2, Yb (2), x = 1, Eu (3), x = 2, Dy (4), x = 1, Tb (5), x = 2} synthesized by Ln(NO₃)₃·nH₂O and ligand (L) in a 1:1 M ratio in ethanol. All the reported compounds are very stable at room temperature, non-hygroscopic. These complexes are insoluble in methanol, chloroform, benzene and soluble in DMSO, DMF and THF.

3.1. Infrared spectra

The infrared vibrations are very important in the structure elucidation of complexes. The representative IR spectra of Schiff base ligand and their Nd(III) (1) complex have been presented in (Fig. S1). The free ligand revealed a significant band at 1630 cm⁻¹ that corresponds to azomethine (C=N) moiety [32]. This band indicates a lower wavenumber shift and appears at 1597 cm⁻¹ in complex because of the manipulation of the nitrogen atom with metal center [33,34]. This observation was also supported by the appearance of a new medium intensity group at 468 cm⁻¹ because of Nd ← N extending vibration [35].

A wide absorption band observed at 3320 cm⁻¹ on account of the phenolic (OH) group in ligand was found absent in the Ln(III) complexes. The disappearance of the OH group in Ln(III) complex suggests deprotonation of phenolic hydrogen and coordination of oxygen with Nd(III). This coordination was further substantiated by the appearance of the phenolic (C-O) group at lower wavenumber 1437 cm⁻¹ in complex compared to the ligand and appearance of the band at 547 cm⁻¹ due to Nd ← O in the Nd(III) complex [36]. The stretching vibration frequencies of coordinated water [37] appeared in the region 3390–3530 cm⁻¹ in complexes. The band at 3294 cm⁻¹ was ascribed to (NH) in ligand and this band remained unchanged in the spectrum of Nd(III) complex, which indicates the no participation of (NH) group in the complexation [20]. The bands in the ligand due to ν_{as}(SO₂) and ν_s(SO₂) appeared at 1360 and 1157 cm⁻¹, respectively [38] remain unchanged in the complexes indicative that this group is not coordinating with a metal center. This is further supported by the unchanged absorption band of ν(S-N) and ν(C-S) groups appear at 971 and 835 cm⁻¹ in the ligand, respectively [39,40]. The wavenumber of coordinated nitrates in Nd(III) complex was observed at 1494 (ν₁), 1035 (ν₂), 820 (ν₃) and 1287 (ν₄). Besides, the frequency gap between the two highest frequencies band (ν₁.ν₄) approximately appears at 207 cm⁻¹ consistent with the value reported in the literature that the coordinated NO₃⁻ ion in the complex is a bidentate ligand [41]. The IR spectra of the other complexes are almost similar to those of Nd(III) complex. This indicates that all Ln(III) complexes have similar structures where ligand coordinated to metal center in a bidentate N O donor capacity.

3.2. UV-Vis spectra

The UV-Vis spectra of ligand (L) and their lanthanide complexes (1–5) were measured in the concentration of 10⁻⁴ mol/L using a DMSO solvent at room temperature (Fig. 1). The ligand shows mainly three absorption bands at 380, 435 and 457 nm [42]. The band at 380 nm is due to π → π* transition within the aromatic ring. The absorption band at 440 and 462 nm of ligand, are assigned to n → π* transition between lone pair electron of azomethine (C=N) group and a conjugated π bond of the aromatic unit [43,44]. The absorption spectra of complexes are similar to each other which concern resemblance in the structures of complexes. The absorption bands at the presence of Ln(III) ions had slight change and variable decrease in the intensity as compared to the free ligand which indicates that the ligand has been the energy donor in addition to the luminescence sensitizer of Ln(III) ions [45]. Lanthanide ions do not lead to the absorption spectra of the complexes [46], considering that f-f transition is Laporte forbidden. They are supposed to be weak due to the low molar absorption coefficient in the UV-Visible region.

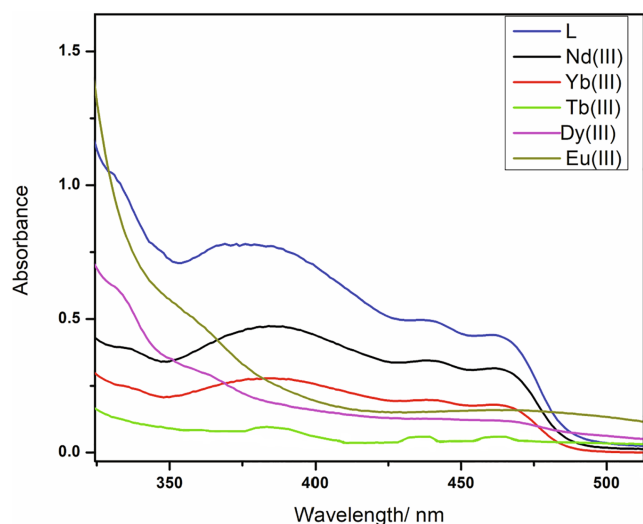


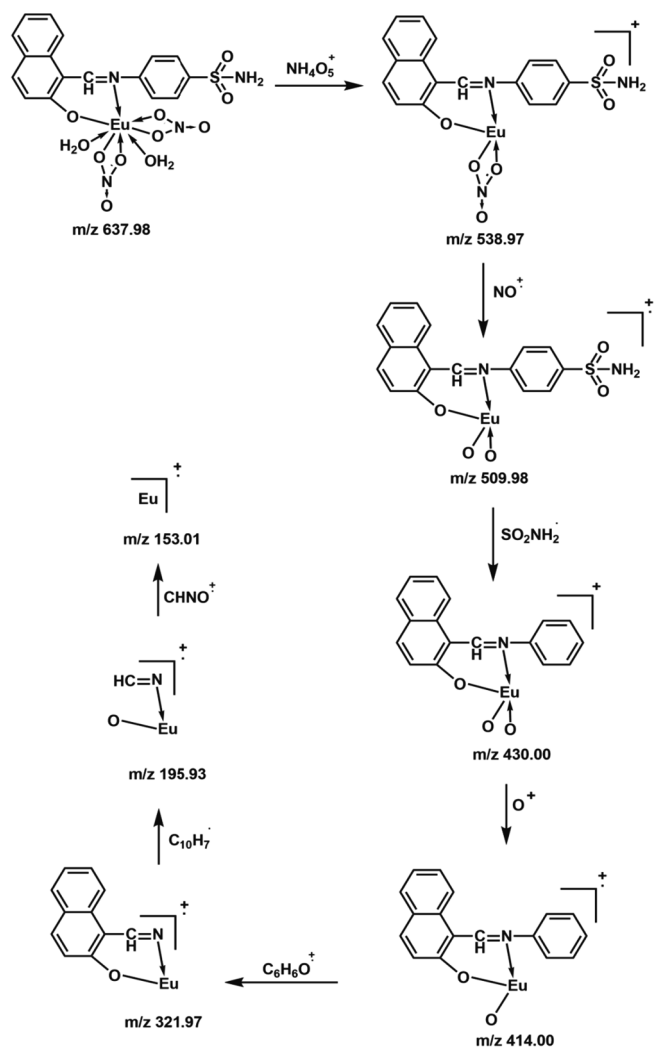
Fig. 1. UV-Vis absorption spectra of Schiff base ligand (L) and their Ln(III) complexes.

3.3. Molar conductance

The Λ_m values of the Ln(III) complexes in DMF solution at 25 °C were estimated. The conductance of prepared complexes is in the range reported for 1:1 electrolytes reveals that two nitrate ions occupy the inner coordination sphere [47]. This is further supported by the results obtained from IR and TGA analysis.

3.4. Mass spectrometry

The TOF-MS ES + spectral data of ligand (L) and its lanthanide compounds (1–5) were recorded and fragmentation patterns with m/z have been indicated. The mass spectra of ligand (L) and their Ln(III) complexes were displayed in (Fig. S2). The group of peaks observed in the spectra of complexes is due to isotopes of metals. In the spectra of complexes, the molecular ion peaks were observed at m/z 327.42 (calcd. 326.07), 625.42 (calcd. 626.87), 658.11 (calcd. 659.00), 636.73 (calcd. 637.98), 648.23 (calcd. 648.99), and 633.09 (calcd. 634.99) due to $[C_{17}H_{14}N_2O_3S]$ (L), $[C_{17}H_{17}N_4O_{11}SNd]$ (1), $[C_{17}H_{17}N_4O_{11}SYb]$ (2), $[C_{17}H_{17}N_4O_{11}SEu]$ (3), $[C_{17}H_{17}N_4O_{11}SDy]$ (4) and $[C_{17}H_{17}N_4O_{11}STb]$ (5), respectively. In the spectra of Ln(III) complexes the base peak observed due to fragments $(C_{17}H_{17}LnN_2O_5S)^+$ at m/z 500.89 (calcd. 502.99) (1), $(C_{17}H_{17}YbN_2O_5S)^+$ at m/z 533.86 (calcd. 535.02) (2), $(C_{17}H_{17}EuN_2O_5S)^+$ at m/z 511.25 (calcd. 514.01) (3), $(C_{17}H_{17}DyN_2O_5S)^+$ at m/z 521.89 (calcd. 525.01) (4) and $(C_{17}H_{17}TbN_2O_5S)^+$ at m/z 516.36 (calcd. 520.01) (5), respectively. All the Ln(III) complexes contain different peaks observed at m/z 422.07 (calcd. 423.01) and 219.95 (calcd. 220.93) due to formation of different fragments $(C_{17}H_{15}NNdO_3)^+$ and $(CH_3NdNO_3)^+$ in (1), at m/z 453.34 (calcd. 455.04) and 231.06 (calcd. 234.96) due to formation of different fragments $(C_{17}H_{15}YbNO_3)^+$ and $(CH_3YbNO_2)^+$ in (2), at m/z 433.18 (calcd. 434.03) and 215.01 (calcd. 213.94) due to formation of different fragments $(C_{17}H_{15}EuNO_3)^+$ and $(CH_3EuNO_2)^+$ in (3), at m/z 443.88 (calcd. 454.03) and 221.45 (calcd. 224.95) due to formation of different fragments $(C_{17}H_{15}DyNO_3)^+$ and $(CH_3DyNO_2)^+$ in (4), whereas in complex (5) these peaks observed at m/z 438.43 (calcd. 440.03) and 218.73 (calcd. 219.94) due to formation of different fragments $(C_{17}H_{15}TbNO_3)^+$ and $(CH_3TbNO_2)^+$. The different fragmentation pattern of europium complexes (Fig. S2) has been suggested in Scheme 2.



Scheme 2. Fragmentation pattern of Eu(III) (3) derived from the TOF-MS spectrum.

3.5. Computational studies

Several attempts have been made to acquire a single crystal for X-rays studies but unfortunately, we did not get an appropriate crystal. In the absence of a suitable single crystal for crystallographic studies, the computation calculation became significant. The computational investigation helps in the authentication of experimental observation with theoretical data. The molecular geometry suggested by different experimental analysis was compared with the ground state optimized geometry. The optimized ground state geometry was calculated by using the DFT/B3LYP-SDD (d, f) method was illustrated in (Fig. 2). The dipole moment, optimized energy and energy bandgap values are summarized in Table 1. The molecular structure of ligand and their neodymium, ytterbium complexes with the atom labeling scheme was shown in (Fig. S3) and selected bond length and bond angle were summarized in Table 2. Theoretically calculated values of important bond lengths (Ln–O, Ln ← N, –C=N) and bond angles were compared with X-ray crystallographic data of the similar type of lanthanide complexes and it was found in a very close agreement [48]. The stability of complexes concerning ligand can also be predicted by observing the energy gap of HOMO and LUMO. The HOMO (highest occupied molecular orbital) energy reflects the capability to contribute an electron while the LUMO (lowest unoccupied molecular orbital) as an electron acceptor signifies the capability to get an electron. The HOMO and LUMO of ligand and their Nd(III) (1) and Yb(III) (2) complexes are

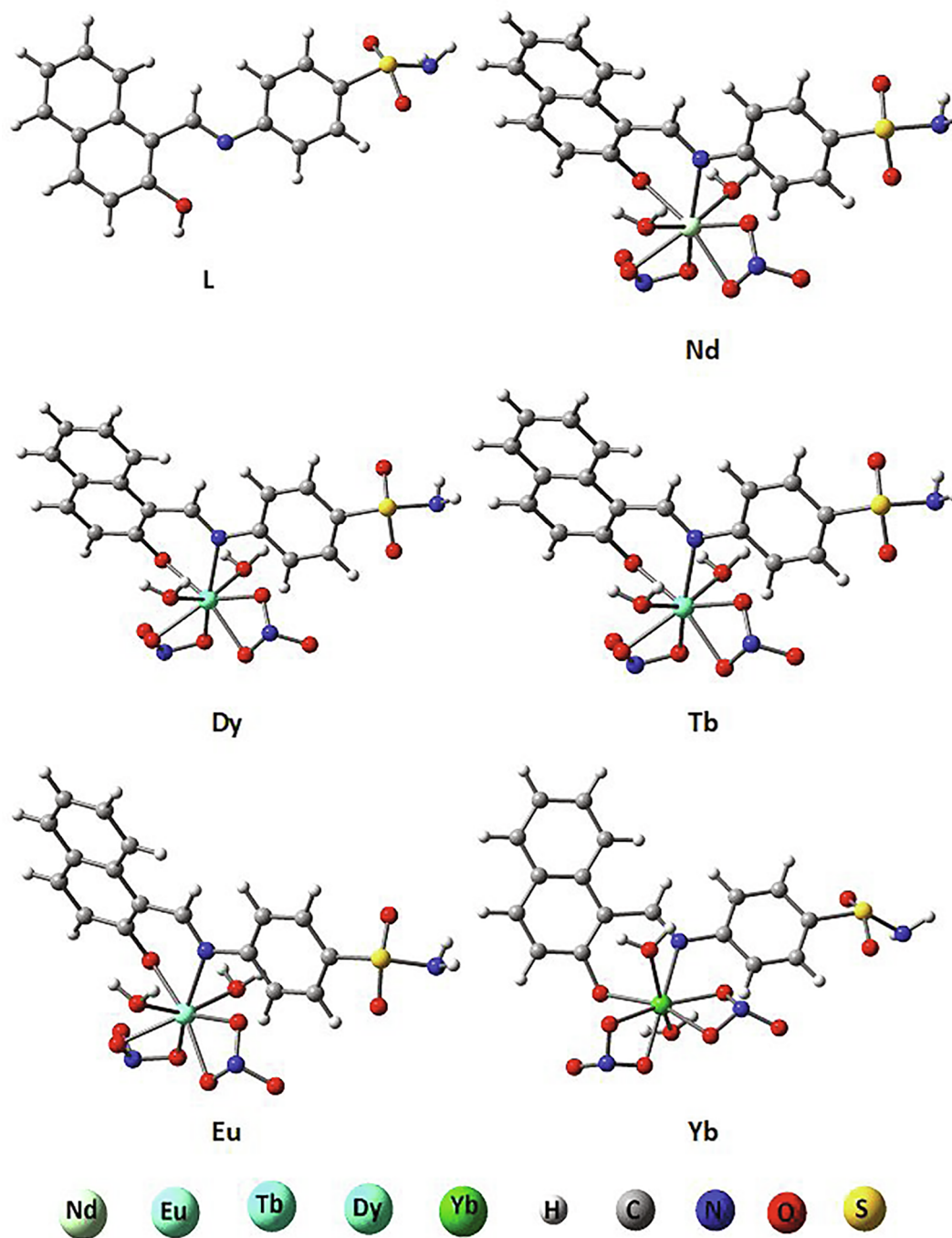


Fig. 2. The optimized ground state geometry of the ligand (L) and their Ln(III) complexes at the B3LYP/SDD (d, f) level of theory.

shown in (Fig. 3). The reactivity and stability of the complexes are related to the energy bandgap. The obtained energy gap (ΔE) values of optimized Ln(III) complexes suggest that the ytterbium complex is less stable than the neodymium complex.

3.6. Fluorescence study

The fluorescence properties of Ln(III) complexes (1.0×10^{-5} M in DMSO) were analyzed at room temperature and spectra of the complexes were obtained upon excitation at 300 nm. The fluorescence

Table 1
Computed electronic properties of Schiff base ligand (L) and their Ln(III) complexes.

S. No.	Compound	Total energy (eV)	Dipole moment (D)	HOMO (eV)	LUMO (eV)	HOMO-LUMO Energy gap (eV)
1.	L	-37,806.87	5.38	-6.25	-2.67	-3.58
2.	Nd(III) (1)	-72,434.51	25.20	-15.95	-15.35	-0.60
3.	Yb(III) (2)	-88,705.87	26.38	-16.03	-15.51	-0.52

Table 2
Selected structural parameters for ligand (L), Nd(III) (1) and Yb(III) (2) at DFT/B3LYP level of theory.

Complexes	Bond length (Å)		Bond angle (°)	
(L)	19C = 21N	1.312	170-14C-11C	121.919
	21N-22C	1.416	170-14C-15C	116.850
	22C-24C	1.408	14C-11C-19C	119.298
	22C-23C	1.407	4C-11C-19C	121.802
	19C-11C	1.438	11C-19C-21N	122.156
	11C-4C	1.451	19C-21N-22C	122.780
	11C-14C	1.413	21N-22C-23C	117.673
	14C-17O	1.357	21N-22C-24C	122.702
	Nd(III) (1)	31Nd-19N	2.334	31Nd-40O-50N
19N = 18C		1.294	31Nd-38O-50N	95.957
31Nd-44O		2.299	40O-50N-51O	113.595
31Nd-17O		2.290	44O-31Nd-19N	77.631
31Nd-41O		2.299	44O-31Nd-17O	65.891
31Nd-38O		2.305	19N-31Nd-41O	67.678
31Nd-40O		2.305	19N-31Nd-17O	80.848
38O-50N		1.352	19N-31Nd-40O	128.490
1C-17O		1.433	19N-31Nd-39O	89.437
Yb(III) (2)		51Yb-19N	2.334	43O-51Yb-19N
	19N = 18C	1.294	43O-51Yb-17O	65.891
	51Yb-43O	2.299	43O-51Yb-40N	144.061
	51Yb-17O	2.290	17O-51Yb-19N	80.848
	51Yb-39O	2.305	51Yb-39O-49N	96.039
	17O-1C	1.433	51Yb-37O-49N	95.957
	51Yb-37O	2.305	19N-51Yb-39O	128.490
	37O-49N	1.352	19N-51Yb-37O	171.025
	49N-50O	1.360	43O-51Yb-37O	94.394

emission bands of the Ln(III) complexes have been exemplified in Table 3. A characteristic emission band was observed approximately at 490 nm in neodymium, ytterbium and approximately at 425 nm in europium, dysprosium and terbium complexes, attributed to $\pi^* \rightarrow \pi$ electron transitions of the aromatic Schiff base ligand [49] (Fig. 4). The luminescent properties of lanthanide complexes are due to the intramolecular energy transfer from the lowest energy level of the triplet state of the organic ligand to the resonance energy level of the lanthanide ions [50]. The augmentation of luminescence intensity is based on the essence of the lanthanide ion that was in the order $\text{Eu(III)} > \text{Dy(III)} > \text{Tb(III)} > \text{Yb(III)} > \text{Nd(III)}$ [51]. Upon the excitation, Nd(III) (1) complex exhibit three characteristic emission peaks in the region 490–700 nm corresponding to $\pi^* \rightarrow \pi$ (490 nm), ${}^4G_{7/2} \rightarrow {}^4I_{9/2}$ (550 nm)

Table 3
Fluorescence spectral data of Ln(III) complexes in DMSO solution at room temperature.

S. No.	Compound	λ_{exc} (nm)	$\nu(\text{cm}^{-1})$	λ_{em} (nm)	Assignment
1.	Nd(III) (1)	300	33,333	490	$\pi^* \rightarrow \pi$
				550	${}^4G_{7/2} \rightarrow {}^4I_{9/2}$
				695	${}^4G_{5/2} \rightarrow {}^4I_{9/2}$
2.	Eu(III) (3)	300	33,333	440	$\pi^* \rightarrow \pi$
				545	${}^5D_0 \rightarrow {}^7F_1$
				695	${}^5D_0 \rightarrow {}^7F_2$
3.	Dy(III) (4)	300	33,333	482	$\pi^* \rightarrow \pi$
				545	${}^4F_{9/2} \rightarrow {}^6H_{13/2}$
				695	${}^4F_{9/2} \rightarrow {}^6H_{13/2}$
4.	Tb(III) (5)	300	33,333	490	$\pi^* \rightarrow \pi$
				545	${}^5D_4 \rightarrow {}^7F_5$
				593	${}^5D_4 \rightarrow {}^7F_4$
				691	${}^5D_4 \rightarrow {}^7F_3$

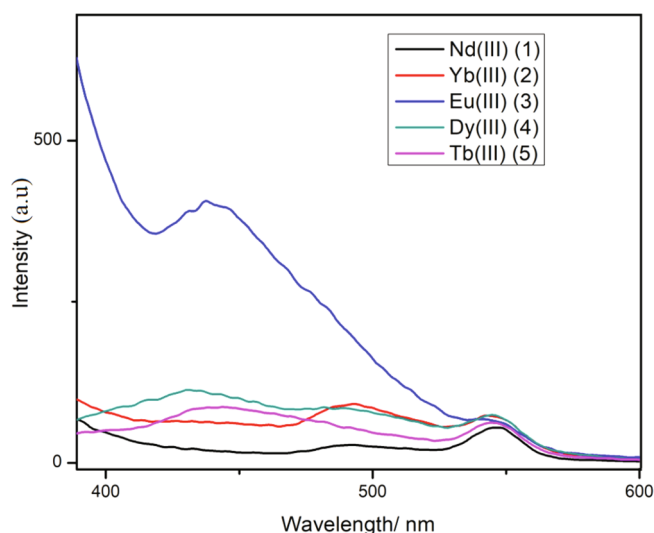


Fig. 4. Emission spectra of lanthanide complexes at $\lambda_{\text{exc}} = 300$ nm in DMSO solution (1.0×10^{-5} M) at room temperature.

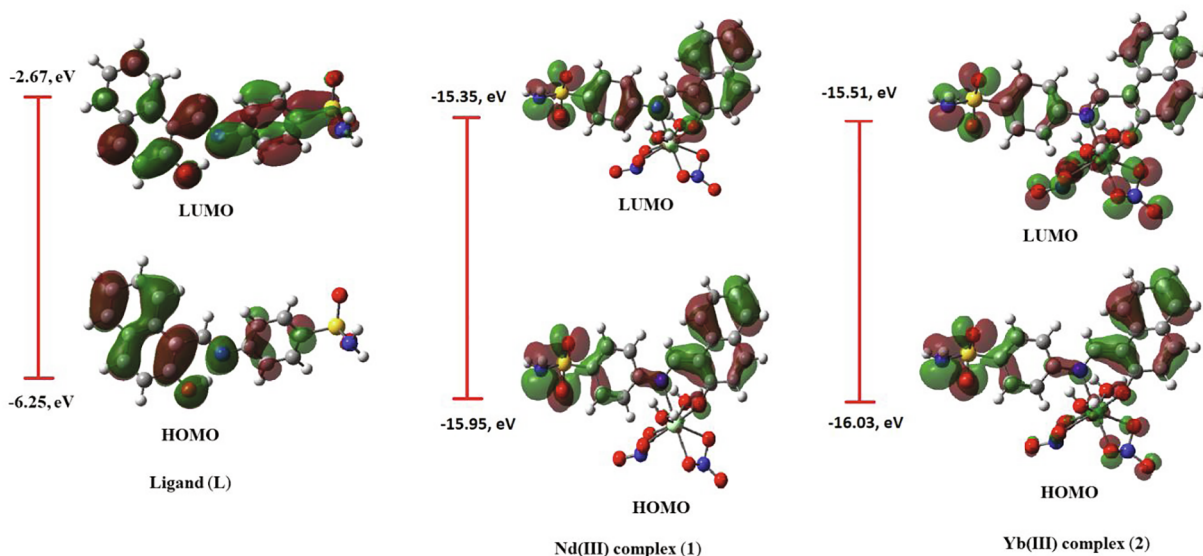


Fig. 3. Energy diagram of frontier molecular orbitals HOMO and LUMO of ligand (L), Nd(III) (1) and Yb(III) (2) complexes derived from DFT calculations using B3LYP/SDD (d, f) level of theory.

and ${}^4G_{5/2} \rightarrow {}^4I_{9/2}$ (695 nm), transitions [45,52]. The Eu(III) (3) complex displays three characteristic peaks in the region 440–708 nm. These emission peaks are attributed to $\pi^* \rightarrow \pi$ (440 nm), ${}^5D_0 \rightarrow {}^7F_1$ (545 nm) and ${}^5D_0 \rightarrow {}^7F_2$ (695 nm), transitions. In Dy(III) (4) complex three narrow emission peaks are observed in the range of 482–700 nm which is attributed to $\pi^* \rightarrow \pi$ (482 nm), ${}^4F_{9/2} \rightarrow {}^6H_{13/2}$ (545 nm) and ${}^4F_{9/2} \rightarrow {}^6H_{11/2}$ (695 nm), transitions [53]. The Tb(III) (5) complex exhibits four emission peaks in the range of 490–691 nm attributed to $\pi^* \rightarrow \pi$ (490 nm), ${}^5D_4 \rightarrow {}^7F_5$ (545 nm), ${}^5D_4 \rightarrow {}^7F_4$ (593 nm), ${}^5D_4 \rightarrow {}^7F_3$ (691 nm), transitions [32]. Inspection of Nd(III), Yb(III), Eu(III), Dy(III) and Tb(III) complexes exhibit the characteristic emission spectra of the Ln(III) ions, respectively, which concern ligand act as good organic chromophore that can be used to absorb and transfer energy to the Ln(III) ions (Fig. S4).

3.7. Thermal behavior

The thermal study of ligand (L) and Eu(III) (3), Dy(III) (4) and Tb(III) (5) complexes were performed under nitrogen atmosphere in the temperature range from 30 to 700 °C (Fig. S5). TGA results showed that ligand is thermally stable in the temperature range from 30 to 185 °C. The decomposition start at 185 °C and completed at 700 °C with two decomposition steps. A sharp endo peak observed in DTA curve around 272 °C may be due to loss of moisture and other two endo peaks around 315 °C and 505 °C due to loss of ligand [54,55]. The thermal behaviors of all the complexes are almost same. The comparative TGA scans of ligand and their lanthanide complexes were shown in (Fig. 5). The coordinated water and lattice water molecules was decomposed below 100 °C with a good agreement between the calculated and found values (11.30% calcd, 12.01% found for Eu(III); 11.11% calcd, 11.51% found for Dy(III); 8.51% calcd, 9.77% found for Tb(III)). The coordinated nitrate molecules decomposed around 300 °C with a weight loss of (19.46% calcd, 19.81 found for Eu(III); 19.13% calcd, 20.23 found for Dy(III); 19.55% calcd, 16.33% found for Tb(III)). A major level decomposition occurred with temperature range from 300 to 700 °C due to loss of organic moiety with the weight loss of about 25.86% for Eu(III); 29.74% for Dy(III) and 36.80% for Tb(III) complexes. Finally, these processes were followed by the last step, in which, oxidation of Ln(III) complexes occurs to give the corresponding oxide as residue [56].

3.8. Antibacterial activity

The result of antibacterial action of ligand (L), Eu(III) (3), Dy(III) (4)

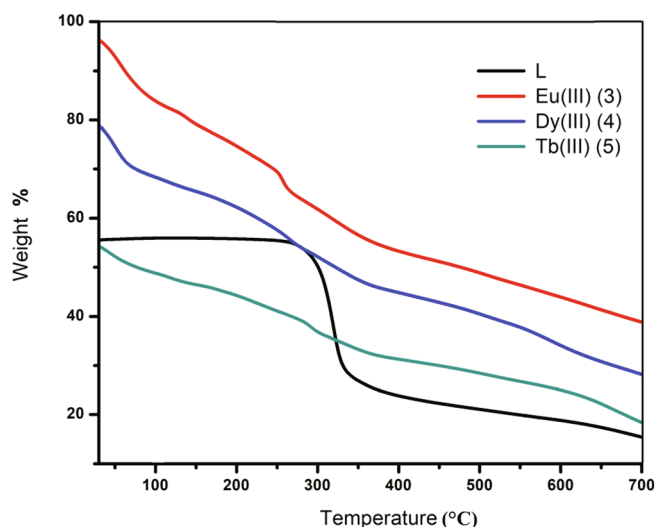


Fig. 5. The comparative TGA-DTA curve of ligand (L) and their Ln(III) complexes.

and Tb(III) (5) complexes have been outlined in Table 4. The result specifies that ligand shows moderate activity against *S. aureus*, *K. pneumoniae* and *P. aeruginosa* with MIC 32 µg/mL and no activity against *E. Coli* as well as *A. baumannii* (MIC > 64 µg/mL). The Dy(III) and Tb(III) complexes showed high activity against *S. aureus* with MIC 16 µg/mL. Eu(III) complex showed less activity against *S. aureus* and no activity against *E. coli*, *K. pneumoniae*, *A. baumannii* and *P. aeruginosa*. The Dy(III) complex demonstrated moderate activity against *E. coli*, *A. baumannii* and *P. aeruginosa* with MIC 32 µg/mL and less activity against *K. pneumoniae*. The complex Tb(III) exhibits less activity against *P. aeruginosa* and no action against *E. coli*, *K. pneumoniae* and *A. baumannii*. The activity of these compounds was compared with standard antibiotic *levofloxacin*, which shows that these complexes have less activity compared to the standard drug. The larger activity of Ln(III) complexes as compared to Schiff base ligand could be described on the basis of Overtone's concept [57] and Tweedy's chelation theory [58]. This theory concern delocalization of π -electrons in the whole chelate ring because of this positive charge at metal ions reduces and the lipophilic character of metal chelate rises, which favors its permeation over the lipid layer of bacterial membranes [59].

4. Conclusion

A sulfanilamide and naphthaldehyde derivative ligand was synthesized and characterized. The bidentate N O donor Schiff base ligand was used to synthesize five new lanthanide (III) complexes with Nd, Yb, Eu, Dy and Tb. The structure of newly synthesized complexes were determined by elemental analysis, molar conductance, FT-IR, UV-Vis spectroscopy and mass spectrometry as well as TGA technique. The experimental investigation supports mononuclear 1:1 metal to ligand ratio with eight coordination central metal ion in lanthanide complexes. The optimized ground state geometries of complexes by DFT calculations further validates the coordination of metal center. The antibacterial studies reported in form of MIC value which show moderate to low activity of lanthanide complex. The emission spectra of complexes indicated the luminescence properties of all lanthanide complexes due to lanthanide ions present at the center.

CRediT authorship contribution statement

Sikandar Paswan: Methodology, Conceptualization, Investigation, Writing - original draft, Funding acquisition, Resources. **Nitesh Jaiswal:** Formal analysis, Writing - review & editing. **Vishnu Kumar Modanawal:** Methodology, Visualization. **Manoj Kumar Patel:** Methodology, Resources. **Rana Krishna Pal Singh:** Supervision, Conceptualization.

Declaration of Competing Interest

The authors declare that they have no known competing financial interests or personal relationships that could have appeared to influence the work reported in this paper.

Acknowledgments

We gratefully acknowledge the Department of Chemistry, University of Allahabad, Allahabad, for providing laboratory facilities. The author (Sikandar Paswan) is very thankful to UGC, New Delhi for financial support in the form of senior research fellowship (SRF). The authors also acknowledge CDRI Lucknow for antibacterial screening, MRC-MNIT Jaipur for IR, Mass, fluorescence analysis and BHU Varanasi for TGA and UV-Vis analysis.

Table 4
Minimum Inhibitory Concentration (MIC) of Schiff base ligand (L) and their Ln(III) complexes.

Sr. No.	Compound	MIC ($\mu\text{g/mL}$)				
		Gram – ve				Gram + ve
		<i>E. Coli</i>	<i>P.aeruginosa</i>	<i>K.pneumoniae</i>	<i>A.baumannii</i>	<i>S. aureus</i>
1.	DMSO	0.0	0.0	0.0	0.0	0.0
2.	L	> 64	32	32	> 64	32
3.	Eu(III) (3)	> 64	> 64	> 64	> 64	64
4.	Dy(III) (4)	32	32	64	32	16
5.	Tb(III) (5)	> 64	64	> 64	> 64	16
6.	Levofloxacin ^a	0.0156	1	64	8	0.25

^a standard drug.

Appendix A. Supplementary data

Supplementary data to this article can be found online at <https://doi.org/10.1016/j.ica.2020.119955>.

References

- [1] P. Yan, W. Sun, G. Li, C. Nie, T. Gao, Z. Yue, J. Coord. Chem. 60 (18) (2007) 1973.
- [2] Y. Wang, H. Li, L. Gu, Q. Gan, Y. Li, G. Calzaferri, Microporous Mesoporous Mater. 121 (2009) 1.
- [3] S. Prochazkova, J. Hranicek, V. Kubicek, P. Hermann, Polyhedron 111 (2016) 143.
- [4] X. Yang, R.A. Jones, S. Huang, Coord. Chem. Rev. 273 (2014) 63.
- [5] S.D. Han, X.H. Miao, S.J. Liu, X.H. Bu, Inorg. Chem. Front. 1 (7) (2014) 549.
- [6] R.M. Wen, S.D. Han, G.J. Ren, Z. Chang, Y.W. Li, X.H. Bu, Dalton Trans. 44 (24) (2015) 10914.
- [7] H. Zhou, Y. Jiang, M. Chen, Y. Wang, Y. Yao, B. Wu, D. Cui, J. Organomet. Chem. 763 (2014) 52.
- [8] M.N. Gueye, M. Dieng, I.E. Thiam, D. Lo, A.H. Barry, M. Gaye, P. Retailleau, S. Afr. J. Chem. 70 (2017) 8.
- [9] A.M. Ajlouni, Q.A. Salem, Z.A. Taha, A.K. Hijazi, W.A. Momani, J. Rare Earths 34 (10) (2016) 986.
- [10] X.I. Hongzhen, L.U. Guanzhong, J. Rare Earths 31 (6) (2013) 639.
- [11] P. Nagpal, R.V. Singh, App. Organomet. Chem. 18 (5) (2004) 221.
- [12] A. Kolaczek, I. Fusiarsz, J. Lawecka, D. Branowska, Chemik 68 (7) (2014) 620.
- [13] J.A. Kovacs, C.J. Allegra, J. Beaver, D. Boarman, M. Lewis, J.E. Parrillo, B. Chabner, H. Masur, J. Infect. Dis. 160 (2) (1989) 312.
- [14] G.M. Rishton, D.M. Retz, P.A. Tempest, J. Novotny, S. Kahn, J.J. Treanor, J.D. Lile, M. Citron, J. Med. Chem. 43 (12) (2000) 2297.
- [15] C.M. Sharaby, Spectro Acta, Part A 66 (4–5) (2007) 1271.
- [16] (a) C.Y. Wu, L.H. Chen, W.S. Hwang, H.S. Chen, C.H. Hung, J. Organomet. Chem. 689 (13) (2004) 2192; (b) H.L. Singh, S. Varshney, A.K. Varshney, Appl. Organomet. Chem. 13 (9) (1999) 637.
- [17] (a) N. Sahu, D. Das, S. Mondal, S. Roy, P. Dutta, N. Sepay, S. Gupta, E.L. Torres, C. Sinha, New J. Chem. 40 (6) (2016) 5019; (b) S. Mondal, T.K. Mondal, Y. Rajesh, M. Mandal, C. Sinha, Polyhedron 151 (2018) 344.
- [18] (a) M. Shakir, A. Abbasi, M. Faraz, A. Sherwani, J. Mol. Struct. 1102 (2015) 108; (b) G.L. Drisko, C. Sanchez, Eur. J. Inorg. Chem. 2012 (32) (2012) 5097.
- [19] (a) R.K. Dubey, A.P. Singh, N. Jaiswal, D.P. Singh, A.K. Meenakshi, M. Kushwaha, A Anjum Kumar, J. Coord. Chem. 72 (19–21) (2019) 3371; (b) S. Paswan, A. Anjum, A.P. Singh, R.K. Dubey, Indian J. Chem. Sect. A. 58 (2019) 446; (c) S. Paswan, A. Anjum, N. Yadav, N. Jaiswal, R.K.P. Singh, J. Coord. Chem. 73 (4) (2020) 686.
- [20] Z.H. Chohan, H.A. Shad, J. Enzyme Inhib. Med. Chem. 23 (3) (2008) 369.
- [21] S. Mondal, S.M. Mandal, T.K. Mondal, C. Sinha, J. Mol. Struct. 1127 (2017) 557.
- [22] M.J. Frisch, G.W. Trucks, H.B. Schlegel, G.E. Scuseria, M.A. Robb, J.R. Cheeseman, G. Scalmani, V. Barone, B. Mennucci, G.E. Petersson, H. Nakatsuji, Gaussian~ 09 Revision D. 01.
- [23] A. Bergner, M. Dolg, W. Kuchle, H. Stoll, H. Preu, Mol. Phys. 80 (6) (1993) 1431.
- [24] M. Buhl, C. Reimann, D.A. Pantazis, T. Bredow, F. Neese, J. Chem. Theory Comput. 4 (9) (2008) 1449.
- [25] A.D. Becke, J. Chem. Phys. 104 (3) (1996) 1040.
- [26] C. Lee, W. Yang, R.G. Parr, Phys. Rev. B 37 (2) (1988) 785.
- [27] J. Burt, W. Levason, M.E. Light, G. Reid, Dalton Trans. 43 (39) (2014) 14600.
- [28] A.C. Tsipis, Coord. Chem. Rev. 272 (2014) 1.
- [29] P.A. Wayne, Methods for dilution antimicrobial susceptibility tests for bacteria that grow aerobically; approved standard, Ninth Ed. M07-A9.
- [30] J.H. Jorgensen, J.F. Hindler, L.B. Reller, M.P. Weinstein, Clin. Infect. Dis. 44 (2) (2007) 280.
- [31] S. Gatadi, J. Gour, M. Shukla, G. Kaul, A. Dasgupta, Y.V. Madhavi, S. Chopra, S. Nanduri, Eur. J. Med. Chem. 175 (2019) 287.
- [32] O.G. Idemudia, A.P. Sadimenko, A.J. Afolayan, E.C. Hosten, Chem. Aappl. 2015 (2015) 1.
- [33] A. Manimaran, R. Prabhakaran, T. Deepa, K. Natarajan, C. Jayabalakrishnan, Appl. Organomet. Chem. 22 (7) (2008) 353.
- [34] L.U. Yiming, L.I. Shifeng, L.I. Jun, C.H. Xuejuan, T.A. Ruiren, J. Rare Earths 28 (5) (2010) 671.
- [35] Z.A. Taha, A.M. Ajlouni, W.A. Momani, J. Lumin. 132 (11) (2012) 2832.
- [36] L. Lekha, K.K. Raja, G. Rajagopal, D. Easwaramoorthy, J. Mol. Struct. 1056–57 (2014) 307.
- [37] S. Belaid, A. Landreau, S. Djebbar, O.B. Baitich, G. Bouet, J.P. Bouchara, J. Inorg. Biochem. 102 (1) (2008) 63.
- [38] G.R. Burns, Inorg. Chem. 7 (2) (1968) 277.
- [39] R.C. Maurya, P. Patel, Spectrosc. Lett. 32 (2) (1999) 213.
- [40] K. Nakamoto, Infrared Spectra of Inorganic and Coordination Compounds, Wiley, New York, 1970.
- [41] W. Wang, Y. Huang, N. Tang, Spectrochim. Acta Part A 66 (4–5) (2007) 1058.
- [42] G.O. Vellaiswamy, S.E. Ramaswamy, Int. J. Pharm. Pharm. Sci. 6 (1) (2014) 487.
- [43] G. Zhao, Y. Feng, Y. Wen, J. Rare Earths 24 (3) (2006) 268.
- [44] A.A.A. Hussien, W. Linert, Synth. React. Inorg. Met.-Org. Nano-Metal Chem. 39 (9) (2009) 570.
- [45] S. Babu, S. Vidya, K.S.K. Rao, Y.O.I. Lee, J. Chil. Chem. Soc. 62 (2) (2017) 3447.
- [46] Z.A. Taha, A.M. Ajlouni, W.A. Momani, A.A.A. Ghazwi, Spectrochim. Acta Part A 81 (1) (2011) 570.
- [47] W.J. Geary, Coord. Chem. Rev. 7 (1) (1971) 81.
- [48] (a) L. Pavelek, V. Ladanyi, M. Necas, Z. Moravec, K. Wichterle, Polyhedron. 119 (2016) 134; (b) Z.A. Taha, A.M. Ajlouni, T.S. Ababneh, W.A. Momani, A.K. Hijazi, M.A. Masri, H. Hammad, Struct. Chem. 28 (6) (2017) 1907; (c) P. Kalita, A. Malakar, J. Goura, S. Nayak, J.M. Herrera, E. Colacio, V. Chandrasekhar, Dalton Trans. 48 (15) (2019) 4857.
- [49] J.X. Li, Z.X. Du, J. Zhou, H.Q. An, S.R. Wang, B.L. Zhu, S.M. Zhang, S.H. Wu, W.P. Huang, Inorg. Chim. Acta 362 (14) (2009) 4884.
- [50] X. Guo, G. Zhu, Q. Fang, M. Xue, G. Tian, J. Sun, X. Li, S. Qiu, Inorg. Chem. 44 (11) (2005) 3850.
- [51] S. Philip, P.S. Thomas, K. Mohanan, J. Serb. Chem. Soc. 83 (5) (2018) 561.
- [52] A. Seminara, A. Mustumeci, Inorg. Chim. Acta 95 (6) (1984) 291.
- [53] A.M. Ajlouni, Z.A. Taha, K.A.A. Hassan, A.M. Anzeh, J. Lumin. 132 (6) (2012) 1357.
- [54] L. Lekha, K.K. Raja, G. Rajagopal, D. Easwaramoorthy, J. Mol. Struct. 1056 (2014) 307.
- [55] M. Shakir, A. Abbasi, M. Faraz, A. Sherwani, J. Mol. Struct. 1102 (2015) 108.
- [56] S. Khullar, S. Singh, P. Das, S.K. Mandal, ACS Omega 4 (3) (2019) 5283.
- [57] K. Venkateswarlu, N. Ganji, S. Daravath, K. Kanneboina, K. Rangan, Polyhedron 171 (2019) 86.
- [58] A.A.A. Amier, A.A. Kadhum, A.B. Mohamad, Bioinorg. Chem. Appl. 2012 (2012) 1.
- [59] D. Xu, Y. Xu, N. Cheng, X. Zhou, Y. Shi, Q. He, J. Coord. Chem. 63 (13) (2010) 2360.